Matter-antimatter asymmetry of the Universe

András Patkós

Eötvös Loránd Tudományegyetem
Természettudományi Kar
Atomfizikai tanszék

Theory Winter Schhool 2021

February 2, 2021

Outline

Evidence 1: Primordial nucleosynthesis

Evidence 2: Cosmological Microwave Background

Evidence 3: Cosmic observation of antimatter

Strong 1^{st} order EWPT with an extra scalar field

Matter-antimatter separation near the bubble wall

Conclusions

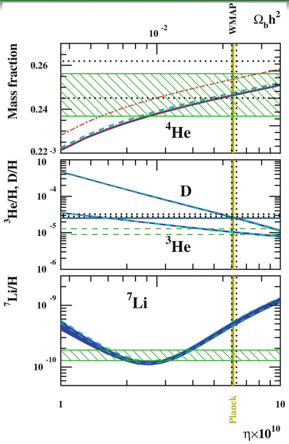

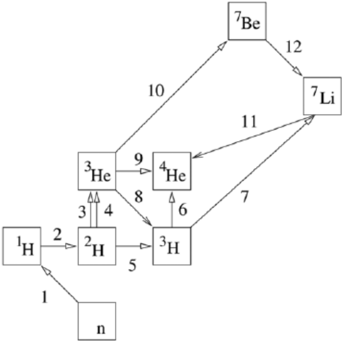

1. $p \longleftrightarrow n$
2. $p(n,\gamma)d$
3. $d(p,\gamma)^3$He
4. $d(d,n)^3$He
5. $d(d,p)t$
6. $t(d,n)^4$He
7. $t(\alpha,\gamma)^7$Li
8. ^{3}He$(n,p)t$
9. ^{3}He$(d,p)^4$He
10. ^{3}He$(\alpha,\gamma)^7$Be
11. ^{7}Li$(p,\alpha)^4$He
12. ^{7}Be$(n,p)^7$Li

Light element abundance

observed, reconstructed

$\eta = \frac{n_B}{s}$

BBN reaction network (12 reactions)

Evidence 1: Primordial nucleosynthesis

- Fractional number density in an ideal nonrelativistic gas mixture:
$$X_i=\frac{n_i}{n_B},\quad \rho_i=\left(M_u+\Delta M_i+\frac{3}{2}T\right)n_i,\qquad p_i=Tn_i$$
$$\rho=\sum_i\rho_i+\rho_{rad}+\rho_\nu+\rho_e,\qquad p=\sum_i p_i+p_{rad}+p_\nu+p_e$$
- Expansion of the Friedmann-Lemaitre Universe:
$$\frac{\dot n_B}{n_B}=-3H,\quad \dot\rho=-3H(\rho+p),\quad H^2=\frac{8\pi G_N}{3}\rho\sim T^4$$
- Nuclear reaction kinetics with laboratory rates:
$$\dot X_i=\sum_{j,k,l}N_i\left(\Gamma_{kl\to ij}\frac{X_l^{N_l}X_k^{N_k}}{N_l!N_k!}-\Gamma_{ij\to kl}\frac{X_i^{N_i}X_j^{N_j}}{N_i!N_j!}\right)$$
- Chemical equilibrium: $n_B\sum_i Z_iX_i=n_{e^-}-n_{e^+}$

Evidence 1: Primordial nucleosynthesis

- Public codes involve reaction channels for isotopes from n, p to $^{15}O,^{16}O$, run in the range $10\mathrm{MeV} > T > 0.01\mathrm{MeV}$.
- D/H varies monotonically with ρ_B e.g. (η),
  produced at $z \sim 10^8$: $p(n,\gamma)D$,
  cosmic evolution: $D(p,\gamma)^3He, D(D,n)^3He, D(D,p)^3H$
  spectroscopically observed at $z \sim 2-3$ in Lyman-α clouds
- Reaction rate sensitivity:
  $$\frac{\Delta(D/H)}{D/H} = -.32\left(\frac{\Delta(\sigma v)}{\sigma v}\right)_{D(p,\gamma)^3He} - .54\left(\frac{\Delta(\sigma v)}{\sigma v}\right)_{D(D,n)^3He} - .46\left(\frac{\Delta(\sigma v)}{\sigma v}\right)_{D(D,p)^3H}.$$
- 1% accuracy for meaningful comparison with observations;
  2020 November: "long awaited and major progress"
  3% accurate measurement of $(\sigma v)_{D(p,\gamma)^3He}$ (LUNA, 2020),
  major contribution from Atomki and Konkoly Observatory[1].

[1] V. Mossa *et al.*, Nature **587** (2020) 210-213

Evidence 1: Primordial nucleosynthesis

- Theory predictions with CMB inputs for deuteron abundance

  $\Omega_B h^2 = 0.02237,\ N_{\nu,eff} = 3.04$ + nuclear reaction rates

  Latest outputs using LUNA2020 for $(D/H)10^5$:
  Pisanti *et al.* (arXiv:2011.11537): 2.54 ± 0.07
  Yeh *et al.* (arXiv:2011.13874): 2.51 ± 0.11
  Pitrou *et al.* (arXiv:2011.11320): 2.439 ± 0.037

- Observed in 7 $Ly\alpha$ clouds (Cooke *et al.*, 2018):

  $$(D/H)_{obs}10^5 = 2.527 \pm 0.030$$

- Increased experimental accuracy results in slight signs for tension among theoretical treatments
- More Lyα clouds should be observed (several thousands are known)

Evidence 2: Cosmic Microwave Background (CMB)

- CMB carries imprints of baryonic matter distribution at $\sim 3.8 \cdot 10^5$yrs ($z \sim 10^3$) following BB, snapshot taken at the moment of photon decoupling from thermal equilibrium

Physics scenario

- Dark Matter forms gravitatonal potential, with fluctuations originating from inflationary quantum fluctuations grown macroscopic
- Baryon-photon plasma before decoupling oscillates in the gravitational potential, reflected by a rich peak-trough structure in the angular decomposition of CMB
- Late evolution of CMB from $z \sim 10^3$ to $z = 0$ is influenced by interaction with matter re-ionised in star formation

Evidence 2: Cosmic Microwave Background (CMB)

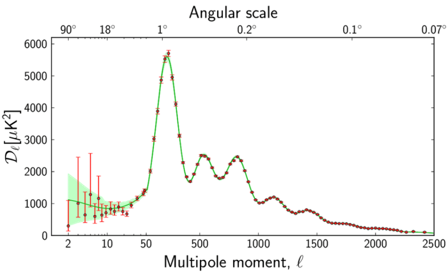

The Planck multipole spectra

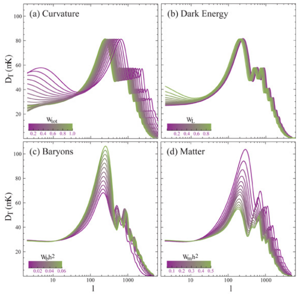

Theoretical reconstruction with dependence on cosmological parameters

Evidence 2: Cosmic Microwave Background (CMB)

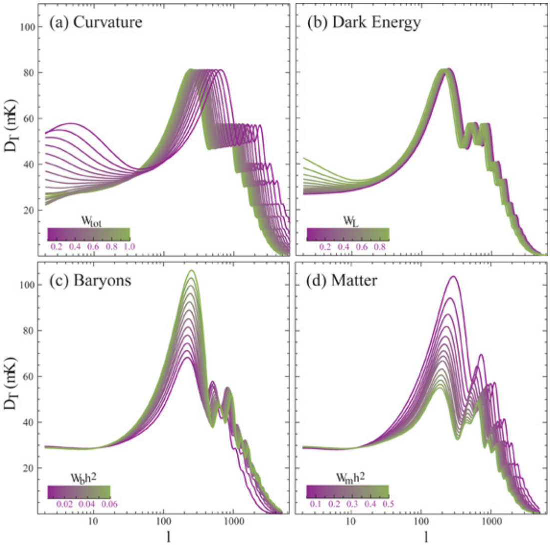

Dependence on cosmological parameters

Directly determined:
A_{curv}, $\Omega_b h^2$, $\Omega_{dm} h^2$
n_s, τ, Θ_{sound}

Derived in ΛCDM model
H_0, Age of Universe,

Evidence 2: Cosmic Microwave Background (CMB)

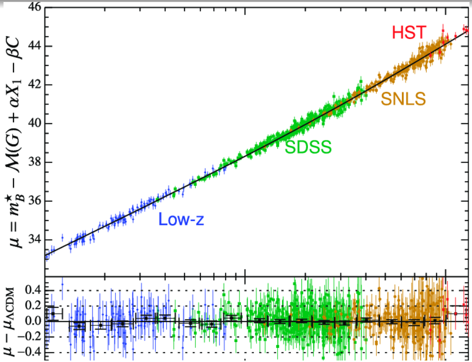

Conflict with other H_0 determinations?

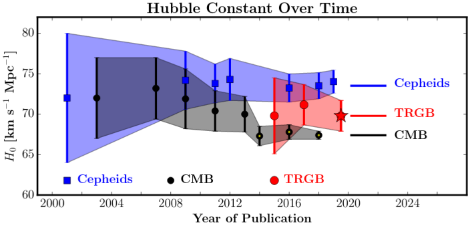

TRGB
= Tip of Red Giant Branch
Carnegie-Chicago project
(W. Freedman)

Evidence 3: Cosmic observation of antimatter

Upper curve: distance $\sim$ 20Mpc, lower curve $\sim$ 1Gpc

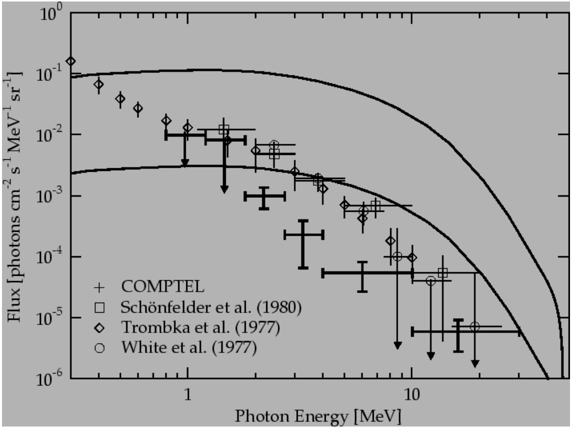

Diffuse gamma background indicates
matter-antimatter boundary farther than 1Gpc
Cohen, de Rujula, Glashow (1998)

Evidence 3: Cosmic observation of antimatter

increased anti-*He* sensitivity of AMS-2 detector on ISS

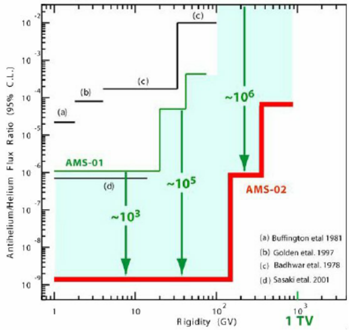

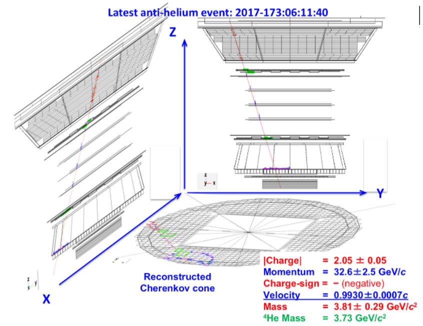

8 events compatible with $\overline{^3He}$ (6) or $\overline{^4He}$ (2) of $E \sim 2-50$GeV
too many(!) compared to $\sim 10^8$ detected ^4He,
? primary cosmic ray, DM annihilation, **anti-clouds, anti-stars** ?

Conclusion on empirical evidence

Status of matter-antimatter asymmetry is solid

At percent level somewhat fluctuating

The most ambitious science story of mankind uniting observations from $z = 0$ to $z = 10^8$

Prelude to Electroweak Baryogenesis: Dimensional reduction

Short reminder: The case of real scalar field
$\phi(\tau, \mathrm{x}) = \frac{1}{\sqrt{\beta V}} \sum_n \sum_{\mathrm{p}} e^{i(\omega_n \tau + \mathrm{px})} \beta \phi_n(\mathrm{p})$.

Gaussian integration in the background of the static $\Phi_0(\mathrm{x})$ mode:

$$-\beta \mathcal{F} = -\frac{\beta}{2} \int_x \left[(\nabla \Phi_0)^2 + m^2 \Phi_0^2 + \frac{\lambda}{4} \Phi_0^4 \right] - \frac{1}{2} \sum_{n,\mathrm{p}} \ln \left[\beta^2 \left(\omega_n^2 + \mathrm{p}^2 + m^2 + 3\lambda \Phi_0^2 \right) \right].$$

High-temperature expansion $m^2 + 3\lambda \Phi_0^2 << T^2$:

$$L_{3D} = \frac{1}{2} \int_x \left[(\nabla \Phi_{3D})^2 + (m_{3D}^2 + \delta m_{3D}^2) \Phi_{3D}^2 + \frac{\lambda_{3D}}{4} \Phi_{3D}^4 \right]$$

$$\Phi_{3D} = \sqrt{\beta} \Phi_0, \quad m_{3D}^2 = m_{ren}^2 + \frac{\lambda_{ren} T^2}{4}, \qquad \lambda_{3D} = T \lambda_{ren}$$

Location of T_c (Landau): $m_{ren}^2 + \frac{\lambda_{ren} T_c^2}{4} = 0$

1-loop solution of 3D theory:

$$\mathcal{F} = \frac{1}{2} m_{3D}^2 \Phi_0^2 + \frac{\lambda_{ren}}{4} \Phi_0^4 - \frac{T}{12\pi} \left(m_{3D}^2 + 3\lambda_{ren} \Phi_0^2 \right)^{3/2}$$

Transition might turn into 1st order due to $\sim \Phi_0^3$ contribution from massless d.o.f.

Strategy 1985-1998 :

Thermally induced cubic potential → 1st order transition[2]

$SU(2)$ invariant Higgs+Gauge theory $V_h = \frac{\lambda h^2}{2}\left(\frac{h^2}{2} - v^2\right) + V_T$

$V_T = \sum_i n_i \left(m_i^2 \frac{T^2}{24} - \frac{T}{12\pi}(m_i^2)^{3/2}\right)$ (n_i: multiplicity of i-th field)

Three massive gauge fields with 3 polarisations, mass $m_i^2 = \frac{g^2 h^2}{4}$:

$$V_h = \left(\frac{3g^2}{32}T^2 - \frac{\lambda v^2}{2}\right)h^2 - \frac{3g^3}{32\pi}Th^3 + \frac{\lambda}{4}h^4$$

$$V_h(T = T_c) = \frac{\lambda}{4}h^2(h - v_c)^2$$

$$\frac{v_c}{T_c} = \frac{3g^3}{16\pi\lambda}, \quad \frac{3g^2}{16}\left(1 - \frac{3g^4}{32\pi^2\lambda}\right)T_c^2 = m_H^2,$$

$$\lambda = 0.13, g = 0.65 \to \frac{v_c}{T_c} \approx 0.13 << 1.1 \text{ (sphaleron washout!)}$$

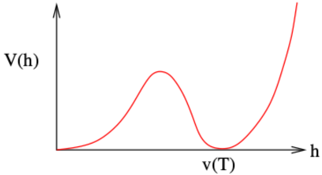

Resummed 1-loop approximation fails: for $m_H > 80$GeV transition becomes crossover! (see Zsolt Szép's lecture!)

[2] Kuzmin, Rubakov, Shaposhnikov, PLB**155** (1985) 36

New strategy 2011[3]:
Two-step transition with classical barrier

$$V_{class} = \frac{\lambda_h}{4}\left(h^2 - v_c^2 + \frac{v_c^2}{w_c^2}S^2\right)^2 + \frac{\kappa}{4}S^2h^2 + \frac{1}{2}(T^2 - T_c^2)(c_h h^2 + c_s S^2)$$

Potentials of extrema at $T = T_c$ (step 2 transition):

$$V_{class}(0,0) = \frac{\lambda_h}{4}v_c^4 > V_{class}(0,w_c) = V_{class}(v_c,0) = 0,$$

Barrier: $V_{class}(v_s,w_s) = \dfrac{\kappa\lambda_h w_c^2 v_c^4}{4\lambda_h v_c^2 + \kappa w_c^2}$,

$$v_s = \frac{2\lambda_h v_c^4}{4\lambda_h v_c^2 + \kappa w_c^2}, \qquad w_s = v_s^2\frac{w_c^2}{v_c^2}$$

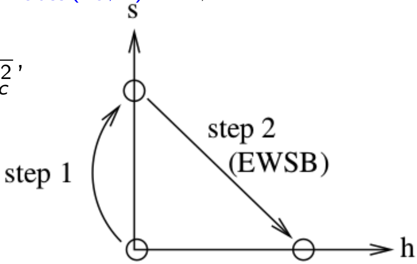

Continuation to $T = 0$
ensuring $V_{class}(0,w_0) > V_{class}(v_0,0)$:

Condition: $\left.\dfrac{\partial V_{class}}{\partial T}\right|_{(v_c,0)} > \left.\dfrac{\partial V_{class}}{\partial T}\right|_{(0,w_c)}$ or $c_h v_c^2 > c_s w_c^2$

[3] J.R. Espinosa *et al.* NPB**854**, 592 (2012)

Parametrisation and renormalisation at $T=0$

$$v_0^2 = v_c^2 + \frac{c_h}{\lambda_h} T_c^2, \quad w_0^2 = w_c^2 + c_s \frac{w_c^4}{v_c^4} \frac{1}{\lambda_h} T_c^2 \qquad v_0 = 246\text{GeV}$$

Quadratic stability of SM vacuum: $c_h > \frac{w_c^2}{v_c^2} c_s$

Spectra:

$$m_S^2 = \frac{1}{2}\left(\lambda_m + \frac{2v_c^2}{w_c^2}\lambda_h\right) v_c^2 + \left(\frac{v_c^2}{w_c^2} - \frac{c_s}{c_h}\right) \frac{c_s}{c_h} T_c^2 > 0$$

$$m_H^2 = 2\lambda_h v_0^2, \qquad m_H = 125\text{GeV}, \qquad m_H << m_S$$

Quartic stability at large (h,s): $\frac{\lambda_h}{|\lambda_m|} > \frac{w_c^2}{2v_c^2}, \quad \lambda_m = \kappa + 2\lambda_h \frac{v_c^2}{w_c^2}$

$$V_{1-loop} = \frac{1}{64\pi^2} \sum_{l=H,S} M_l^4(h,S)\left[\log\frac{M_l^2(h,S)}{Q^2} - C_l\right] + V_{div} + \delta V,$$

$$\delta V = \delta V_0 + \frac{1}{2}\left(\delta\mu_h^2 h^2 + \delta\mu_s^2 S^2\right) + \frac{1}{4}\left(\delta\lambda_h h^4 + \delta\lambda_{hs} h^2 S^2 + \delta\lambda_s S^4\right).$$

Renormalisation conditions at $T = 0$ for $V = V_{class} + V_{1-loop}$

Principle of minimal sensitivity applied

$$\left.\frac{\partial V_{1-loop}}{\partial h}\right|_{(v_0,0)} = \left.\frac{\partial V_{1-loop}}{\partial S}\right|_{(0,w_0)} = 0 \leftrightarrow \text{no change of } v_0, w_0$$

$$\left.\frac{\partial^2 V_{1-loop}}{\partial S^2}\right|_{(v_0,0)} = \left.\frac{\partial^2 V_{1-loop}}{\partial h^2}\right|_{(v_0,0)} = 0 \leftrightarrow \text{unchanged spectra}$$

$$V_{1-loop}|_{(v_0,0)} = V_{1-loop}|_{(0,w_0)} = 0 \leftrightarrow \; V_{class}(T=0) \text{ maintained}$$

Parameters $\lambda_h, v_0, \lambda_m, w_0, T_c$ 2 fixed in the Higgs sector

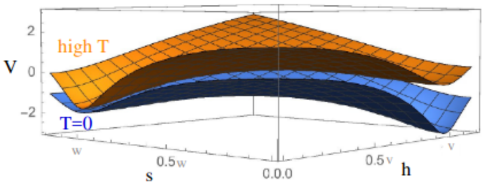

Electroweak Baryogenesis: PT with additional scalar

The potential $V_{T=0,ren}[\lambda_h, v_0, \lambda_m, w_0, T_c] + V_T$

$$V_T = \frac{T^4}{2\pi^2} \sum_{l=B,F} N_l \int_0^\infty dx x^2 \log\left[1 \pm e^{-(x^2+m_l^2/T^2)}\right]$$

$$- \frac{T}{12\pi} \sum_B N_B \left[m_B^2 + c_B T^2\right]^{3/2}$$

Scenario of thermal evolution during the cooling of Universe[4]

- Cooling system starts in the symmetric phase and $Z(2)$ violating transition at $T_S \approx \left(T_c^2 + \frac{\lambda_h}{c_s}\frac{v_c^4}{w_c^2}\right)^{1/2}$. (Step 1)
- Further cooling: 1st order transition to the SM Higgs vacuum at modified transition temperature T_c^{new}. (Step 2, EWBG)
- Bubble nucleation starts at T_{nucl} below T_c (super-cooling)

[4] J.R. Espinosa *et al.* NPB**854**, 592 (2012)

Nucleation temperature T_{nucl}

Nucleation speed per unit volume : $\Gamma_N(T) = T^4 \left(\frac{S_3}{2\pi T}\right)^{3/2} e^{-S_3/T}$

Competing with expansion rate: one bubble in 1 Hubble volume:

$$\frac{4\pi}{3}\frac{1}{H(T_n)^3}\Gamma_N(T_n) \approx H(T_n)$$

The surface energy S_3 in thin wall approximation[5]

$$S_3 = \int_{-\infty}^{\infty} dz \left[\frac{1}{2}\left((\partial_z h)^2 + (\partial_z S)^2\right) + V(h, s, T)\right],$$

$$h(-\infty) = 0, \quad h(\infty) = v(T), \quad S(-\infty) = w(T), \quad S(\infty) = 0$$

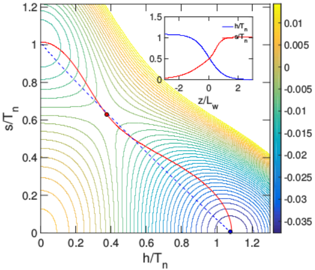

[5] J.M. Cline PRD**95**, 115006 (2017)

Bubble profile (using tree-level potential)[6,7]

Nearby path close to $V_{barrier}$:

$$h(z) = v_c \sin\varphi(z), \quad S(z) = w_c \cos\varphi(z),$$

$$\varphi(z) = \frac{\pi}{4}\left(1 + \tanh\frac{z}{L_w}\right), \quad \varphi(-\infty) = 0, \quad \varphi(\infty) = \frac{\pi}{2}$$

$$V_{class}[\varphi] = \frac{\kappa}{4} v_c^2 w_c^2 \sin^2\varphi \cos^2\varphi, \quad V_{barrier} \approx \frac{\kappa}{16} v_c^2 w_c^2$$

$$S_3 = \frac{\alpha}{L_w}(v_c^2 + w_c^2) + \beta L_w V_{barrier}, \qquad L_w = ?$$

$$\alpha \approx \int_0^{\pi/2} d\varphi\varphi\left(1 - \frac{2\varphi}{\pi}\right), \quad \beta \approx 2\int_0^{\pi/2} d\varphi \sin^2\varphi\cos^2\varphi \frac{1}{\varphi(1-\frac{2\varphi}{\pi})}.$$

Minimisation with respect to L_w:

$$L_w^2 \approx 2.7\frac{v_c^2 + w_c^2}{\kappa v_c^2 w_c^2}\left(1 + \frac{\kappa w_c^2}{4\lambda_h v_c^2}\right).$$

---

[6] J.R. Espinosa *et al.* JCAP 01(2012) 012,

[7] J.M. Cline *et al.* PRD**95** 115006 (2017)

S coupled with massive fermion χ
$\Delta L = \bar{\chi}[i\gamma_\mu\partial^\mu - m_\chi - (mP_R + m^* P_L)S]\chi$

Let $m = i|m|$, then in the bubble wall:
$\Delta L = \bar{\chi}[i\gamma^\mu\partial^\mu - M(z)e^{i\gamma_5\Theta(z)}]\chi$,
$M^2(z) = m_\chi^2 + |m|^2 S^2(z), \qquad \Theta(z) = \arctan\left(\frac{|m|S(z)}{m_\chi}\right)$
$\Theta = \Theta(x)$ cannot be removed by $\psi \to e^{-i\gamma_5\Theta/2}\psi$,
since it reappears in the kinetic term

CP-violation basics CP-transformation, fermions:
$\psi \to i\gamma^2\gamma^0\psi^*, \qquad \psi^\dagger \to \psi^T\gamma^0\gamma^2 i$
Consequence: $\bar{\psi}e^{i\Theta\gamma_5}\psi \to \bar{\psi}e^{-i\Theta\gamma_5}\psi$

$\Theta(z)$: space-dependent CP-violating feature of the construction
$CP[\Theta(z)] = -\Theta(z)$

Matter-antimatter separation near bubble-wall

Semiclassical solution of Dirac equation with complex mass[8,9]:

$m = |m|e^{i\Theta}$

$(i\gamma^\mu\partial_\mu - mP_R - m^* P_L)\psi = (i\gamma^\mu\partial_\mu - me^{i\gamma_5\Theta})\psi = 0$

One-dimensional variation accross the bubble-wall:

$\psi_s = e^{-i\omega t}\begin{pmatrix} L_s \\ R_s \end{pmatrix}\chi_s, \qquad \sigma_3\chi_s = s\chi_s$

$(\omega - is\partial_z)L_s - mR_s = 0, \qquad (\omega + is\partial_z)R_s - m^* L_s = 0$

or

$(\omega + is\partial_z)\frac{1}{m(z)}(\omega - is\partial_z)L_s = 0, \quad (\omega - is\partial_z)\frac{1}{m^*(z)}(\omega + is\partial_z)R_s = 0$

WKB trial wave function:

$L_s = w_L(z)e^{i\int^z p(z')dz'}, \qquad R_s = w_R(z)e^{i\int^z p(z')dz'}$

[8] M. Joyce *et al.*, Phys. Rev. Lett. 75, 1695 (1995)

[9] J. M. Cline *et al.* JHEP 0007, 018 (2000)

Matter-antimatter separation near bubble-wall

Solution for L_s

Real part: $\omega^2 - |m|^2 - p(z)^2 + (s\omega + p)\Theta' - \frac{|m|' w'}{|m| w} + \frac{w''}{w} = 0$

Imaginary part: $2pw' + p' - \frac{|m|'}{|m|}(s + p)w - \Theta' w' = 0$

Perturbative solution assuming slow variation of w, p, Θ

$p^{(0)} = \mathrm{sign}(p)\sqrt{\omega^2 - |m|^2} \equiv p_0,$

$p^{(1)} = \left(p_0^2 + (s\omega + p_0)\Theta'\right)^{1/2} \to p_0 + \frac{s\omega + p_0}{2p_0}\Theta'$

CP-transformed Dirac equation $\Theta \to -\Theta$

$p^{(1)} = p_0 + s_{CP}\frac{s\omega + p_0}{2p_0}\Theta'$

Influence of the phase transformation of $\psi \to e^{i\alpha(z)}\psi$:

$p_L^{(1)} = p_0 + s_{CP}\frac{s\omega}{2p_0}\Theta' + \frac{\Theta'}{2} + \alpha' \equiv p_0 + s_{CP} s \frac{\omega}{2p_0}\Theta' + \alpha_{CP,L}$

Result of the analysis of the equation of R_s:

$p_R^{(1)} = p_0 + s_{CP}\frac{s\omega}{2p_0}\Theta' - \frac{\Theta'}{2} + \alpha' \equiv p_0 + s_{CP} s \frac{\omega}{2p_0}\Theta' + \alpha_{CP,R}$

Dispersion relation: $\omega = \left((p - \alpha_{CP})^2 + |m|^2\right)^{1/2} - s_{CP} s \frac{\Theta'}{2}.$

Canonical equations:

$$v_g = \frac{\partial\omega}{\partial p} = \frac{p_0}{\omega}\left(1 + s_{CP}s\frac{|m|^2}{2p_0^2\omega}\Theta'\right) \equiv \frac{p_{kin}}{\omega}, \qquad \dot{p} = -\frac{\partial\omega}{\partial z}$$

$$\dot{p}_{kin} = \omega\dot{v}_g = \omega(\dot{z}\partial_z v_g + \dot{p}\partial_p v_g)$$

$$F = -\frac{|m||m|'}{\omega} + s_{CP}s\frac{1}{2\omega^2}(|m|^2\Theta')'$$

Second term distinguishes (anti-)fermion with spin projection $s(-s)$ and (anti)-fermion with spin projection $-s(s)$

Boltzmann-equation for the distribution of particles/antiparticles in the neighbourhood of the bubble-wall

$$\dot{f}_i + \frac{p_{kin}}{|m|}\frac{\partial f_i}{\partial z} + \dot{p}_{kin}\frac{\partial f_i}{\partial p_{kin}} = \text{scattering terms}$$

In the frame of the bubble-wall, assuming local thermal equilibrium:

$$\dot{f}_i = 0, \qquad f_i = \left(e^{\beta(\gamma(\omega_i - v_{wall}p_{kin}) - \mu_i)}\right)^{-1} + \delta f_i$$

Matter-antimatter separation near bubble-wall

$\mu_i, \delta f_i$ from the first two moments of the Boltzmann equation

Elimination of δf_i leads to diffusion equations for $\xi_i = \mu_i / T$:

$$-D_i \xi_i'' - v_w \xi_i' + \sum_r \left(\Gamma_r(l + m \to i + j) - \Gamma_r(i + j \to l + m) \right) = S_i$$

CP-dependent source term: $S_i = \dfrac{v_{wall} D_i}{\langle v_g^2 \rangle T} \langle v_g \dfrac{(|m|^2 s_{CP} s \Theta')'}{2\omega^2} \rangle$

Solution with Green's method leads to helicity state separation

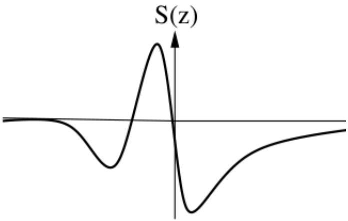

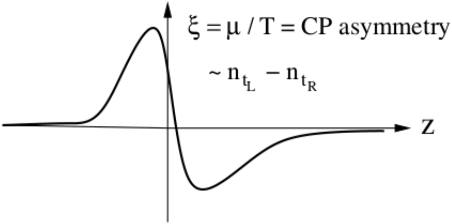

Matter-antimatter separation: model building II.

Transformation into τ-lepton asymmetry by massive Majorana fermion χ coupled with inert scalar dublet ϕ to τ-leptons[10,11]:

$$\Delta L = y\bar{L}_\tau \phi P_R \chi + \mathrm{h.c.}$$

- Helicity state separation in the bubble-wall
- $\chi\tau_L \leftrightarrow \phi$: Helicity asymmetry of χ transfered to $\tau - \bar{\tau}$
- Lepton-asymmetry transfered to quarks through sphaleron mediated processes

[10] J.M. Cline *et al.* PRD**95** 115006 (2017)

[11] j.M. Cline,"Is electroweak baryogenesis dead?", arXiv:1704.08911

Conclusions

- Real scalar field represents a simplest extension of SM possessing sufficient number of new couplings for strong 1st order phase transition
- CP-violating coupling of the scalar to new fermions provides additional strength to matter-antimatter separation in the electroweak bubble wall
- Question for public poll: Is EWBG dead?
- There are other attractive constructions, but experimental guidance for model building is missing!.